All-Order Full-Coulomb Quantum Spectral Line-Shape Calculations

T. A. Gomez, T. Nagayama, P. B. Cho, M. C. Zammit, C. J. Fontes, D. P. Kilcrease, I. Bray, I. Hubeny, B. H. Dunlap, M. H. Montgomery, and D. E. Winget

Phys. Rev. Lett. **127**, 235001 — Published 1 December 2021

DOI: 10.1103/PhysRevLett.127.235001

All-Order Full-Coulomb Quantum Spectral Line-Shape Calculations

T. A. Gomez,[1,*] T. Nagayama,[1] P. B. Cho,[2] M. C. Zammit,[3] C. J. Fontes,[3] D. P. Kilcrease,[3] I. Bray,[4] I. Hubeny,[5] B. H. Dunlap,[2] M. H. Montgomery,[2] and D. E. Winget[2]

[1] *Sandia National Laboratories, Albuquerque, New Mexico 87123, USA*
[2] *University of Texas, Department of Astronomy, Austin, Texas 78712*
[3] *Los Alamos National Laboratory, Los Alamos, New Mexico 87545, USA*
[4] *Curtin Institute of Computation and Department of Physics and Astronomy, GPO Box U1987 Perth, Western Australia 6845, Australia*
[5] *University of Arizona, Department of Astronomy, Tucson, Arizona 85721, USA*

(Dated: November 2, 2021)

Understanding how atoms interact with hot dense matter (HDM) is essential for astrophysical and laboratory plasmas. Interactions in high-density plasmas broaden spectral lines providing a rare window into interactions that govern, for example, radiation transport in stars. However, up to now, spectral line-shape theories employed at least one of three common approximations:2^{nd}-order Taylor treatment of broadening operator, dipole-only interactions between atom and plasma, and classical treatment of perturbing electrons. In this letter, we remove all three approximations for the first time and test the importance for two applications: neutral hydrogen and highly-ionized magnesium and oxygen. We found 15-50% change in the spectral line widths, which are sufficient to impact applications including white-dwarf mass determination, stellar-opacity research, and laboratory plasma diagnostics.

Introduction.— Understanding atomic behavior in hot dense matter (HDM) is essential for understanding astrophysical [1–3] and laboratory [4–6] plasmas but calculations of perturbed atomic structure in the complex environments of HDM plasmas are challenging. High temperature introduces randomness into this perturbation. HDM properties depend on the ensemble average of these random perturbations. This affects ionization and equation of state because the perturbations dissolve atomic states into the continuum, an effect known as ionization-potential depression [7–9]. The perturbations also broaden spectral lines. This leads to convenient plasma diagnostics and affects radiation transport and opacity because photon transport at energies between lines depends on how broad the lines are [1, 10].

Inaccuracies of line-shape models could have consequences in many astrophysics and laboratory plasma physics applications. For example, inconsistencies in Balmer line shapes [11–14] create uncertainties in the determination of white-dwarf masses, which is important for a variety of applications including cosmochronology [15] and type Ia supernovae, and high-density accretion disks around black holes [16, 17]. For laboratory applications, true disagreement between measured and modeled solar iron opacity [18] may be obscured by uncertainties in plasma conditions diagnosed by unverified line shapes [19–21].

There are many competing line-shape models [22–28]; their calculational accuracies are inconclusive due to various untested approximations. Line-shape theory is multidisciplinary, requiring atomic physics, plasma physics, collision physics, and statistical mechanics. There are three common approximations: 2nd-order approximation for the broadening operator, dipole approximation for Coulomb interaction between atoms and plasma particles, and classical approximation for perturbing electrons. Some line-shape calculations remove one or two of the three approximations, but their calculational superiorities are unclear due to the remaining approximation(s). The three aspects, i.e., broadening operator, Coulomb interaction, and treatment of electrons, are fundamentally related, and we cannot fully investigate the importance of one approximation without removing the other two approximations.

Ideally, models would be validated by benchmark experiments [29–33], but since they are few and far between, continued theoretical scrutiny is needed. Benchmark experiments must have uniform plasma conditions with accurate line-shape measurements and independent diagnostics; this is challenging to achieve. Different physics becomes important depending on element, conditions, and transitions, and the existing data are far from sufficient to validate all relevant physics at various conditions. Thus, continued theoretical work aimed at simultaneously removing known approximations is valuable.

Simultaneous removal of the three approximations has been the next step but has not been realized for many decades due to technical challenges, especially because simultaneous removal of 2^{nd}-order and classical approximations has been difficult. All approaches without the 2^{nd}-order approximation [26–28, 34–37] rely on a classical-electron assumption, and there is no easy extension for quantum electrons. All order with quantum electron formulation was introduced in 1963 [23], but has only been evaluated with 2^{nd}order. Incorporation of higher orders significantly complicates the calculation. The path towards simultaneous removal of the three approximations—while critical—has not been clear.

In this letter, we present the first line-shape calculation that simultaneously removes all three approximations by extending our recent work and adopting the technique developed in another field. Our recent work revived the state-of-the-art quantum line-shape calculation [38] and was refined to include missing physics [39]. Adopting a numerical technique used in collision physics [40] helps resolve the longstanding technical problem. These refinements allow us to perform line-shape calculations without the three approximations for the first time. We test the validity of decade-old approximations for K-shell transitions of neutral hydrogen and highly-ionized magnesium and oxygen. We find that, for hydrogen, the 2^{nd}-order approximation overpredicts Lyβ line width by a factor of two at some conditions. Also, classical calculations severely underestimate Lyα line width at low temperatures. Mg Heγ line shapes calculated for stellar-opacity measurements [18, 21] revealed that full-Coulomb interaction was essential for accurate density diagnostics while 2^{nd}-order approximation was found reasonably accurate. Understanding the validity of each approximation is essential for efficient and accurate radiation transport and plasma diagnostics. This work not only significantly advances the line-shape theory but also emphasizes the importance of continued theoretical scrutiny, benchmark experiments, and crosstalk between relevant fields for efficient scientific breakthroughs.

Line-Broadening Fundamentals.—In HDM, the lines are broadened primarily by a radiating atom being perturbed by nearby electrons and ions. Due to the mass differences, ion perturbation is often approximated as a static electric microfield, ϵ. Every atom feels a different microfield, and its probability distribution is denoted by $W(\epsilon)$ and can be calculated by Refs. [41, 42]. The total spectral line shape, $I(\omega)$, is then computed by probability-weighted integration of the electron-broadened line shapes over ϵ [43]:

$$I(\omega) = \Im\frac{-1}{\pi}\int_0^\infty d\epsilon W(\epsilon)\sum_{\beta\beta'\alpha\alpha'}\langle\beta'|D|\alpha'\rangle\langle\alpha|D|\beta\rangle\times \langle\alpha'\beta'|\left[\omega - H(\epsilon) + H^*(\epsilon) - \mathcal{H}(\omega)\right]^{-1}|\alpha\beta\rangle, \quad (1)$$

where $\Im$ denotes the imaginary part; D is the dipole operator of the atom; α, α' and β, β' denote upper and lower states respectively; $H(\epsilon)$ and $H^*(\epsilon)$ are the atomic Hamiltonians for the upper- and lower-state, respectively; and $\mathcal{H}(\omega)$ is the electron-broadening operator.

$\mathcal{H}(\omega)$ is defined as thermal average of collision amplitudes, called T-matrices [22–24]. $\mathcal{H}(\omega)$ contains upper-state, lower-state and interference terms (see Eq. (55) of Fano [23]). For K-shell transitions considered here, the lower-state and interference terms are negligible. The thermal average is calculated by integrating the T-matrix over the perturbing free-electron states, $\mathbf{k}$, weighted by its probability, $f(\mathbf{k})$, (i.e., often Boltzmann):

$$\langle\alpha\beta|\mathcal{H}(\omega)|\alpha'\beta'\rangle = \delta_{\beta\beta'}n_e\int d\mathbf{k}f(\mathbf{k})\langle\alpha\mathbf{k}|T(\omega+E_\beta+E_\mathbf{k})|\alpha'\mathbf{k}\rangle, \quad (2)$$

where n_e is the electron density and $T(\omega+E_\beta+E_\mathbf{k})$ is the T-matrix operator. It is important to note here that the T-matrix has a frequency dependence, which makes the line profile non-Lorentzian and potentially asymmetric. Electron broadening is therefore reduced to the evaluation of the T-matrix, which is formally defined as [44, 45],

$$T(E) = \frac{1}{1 - V(E - H_0)^{-1}}V; \quad (3)$$

This is a function of the energy, $E = \omega + E_\beta + E_\mathbf{k}$, the non-interacting Hamiltonian, H_0, and the atom-electron interaction, V. The V is a screened Coulomb interaction

$$V = \sum_{a=1}^{N}\frac{e^{-|\mathbf{r}_a-\mathbf{r}_p|/\lambda_{\rm scr}}}{|\mathbf{r}_a-\mathbf{r}_p|} - \frac{e^{-|\mathbf{r}_p|/\lambda_{\rm scr}}}{|\mathbf{r}_p|} + V_{\rm Ex}. \quad (4)$$

The first term is the Coulomb repulsion between the N atomic electrons and the perturbing electron. The second is the nuclear potential felt by the perturbing electron. The third contains electron-exchange terms between atomic electron(s) and the perturbing electron [40]. $\lambda_{\rm scr}$ is the screening length [46]. The electron states, $|\mathbf{k}\rangle$, are usually plane waves for neutrals and Coulomb waves for charged radiators.

Approximations.— Here, we elaborate each approximation and explain how we remove these approximations: 2^{nd}-order, dipole, and classical.

2^{nd} order: The calculation of the T-matrix is simplified with a 2^{nd}-order approximation. Since inverting $[1 - V(E - H_0)^{-1}]$ is challenging, it is common to Taylor expand the T-matrix to 2^{nd}order in V,

$$T(E) \approx V + V\frac{1}{E - H_0}V. \quad (5)$$

This approach is accurate only when the interaction V is small.

Dipole: The Coulomb interaction, V, is often approximated by the dot product of the atomic dipole moment with the microfield by the perturbing electrons, $\boldsymbol{\epsilon}_p$ [47, 48],

$$V \approx \sum_{a=1}^{N}\mathbf{r}_a\cdot\boldsymbol{\epsilon}_p; \quad \boldsymbol{\epsilon}_p = \mathbf{r}_p\frac{1}{|\mathbf{r}_p|^3}\left[1 + \frac{|\mathbf{r}_p|}{\lambda_{\rm scr}}\right]e^{-|\mathbf{r}_p|/\lambda_{\rm scr}}. \quad (6)$$

This is called the dipole approximation. While this is a very common approximation for line-shape calculations, its accuracy is not sufficiently studied.

Classical: Perturbing electrons are often treated classically [28, 34, 36, 37, 47, 49]. In this approximation, the perturbing electron wavefunction is replaced by a point particle moving on a classical trajectory, such as

$$\langle\mathbf{r}|\mathbf{k}\rangle = \frac{1}{\sqrt{2\pi}^3}e^{i(\mathbf{k}\cdot\mathbf{r}+E_\mathbf{k}t)} \quad \Rightarrow \quad \mathbf{r}_p(t) = \mathbf{r}_0 + \mathbf{v}t. \quad (7)$$

The accuracy of this approximation becomes questionable at low temperature and high density where quantum effects become important.

While the three approximations (5), (6), and (7) make calculations efficient [47], their potential inaccuracies have been raised repeatedly. For example, 2^{nd}-order approximation does not preserve unitarity of the scattering S-matrix [44]. Ad-hoc strong-collision corrections are introduced to remedy this problem [4, 50], but its accuracy and universality are unknown. The dipole approximation breaks down when the plasma electrons get close to the radiator. However, past investigations on this found conflicting results: Woltz and Hooper [51] found a reduction in the width, Alexiou [52] found an increase in the width, and Junkel *et al.* [53] found additional redshifts. These conflicting results are likely caused by differences in residual approximations. Also, some literature warns that neglected quantum effects [39, 54] may underestimate the broadening. Despite the plausibility of these investigations, the accuracy of their claims is unclear because these investigations were done without removing other fundamentally related approximations. This situation then makes it imperative that a calculation includes all-order (3), full-Coulomb (4), and quantum electrons simultaneously.

We removed all three approximations by extending our recent work and adopting a technique from collision physics. Our previous investigations [38, 39] already removed classical and dipole approximations, leaving only 2^{nd}-order to be removed. Direct inversion of $[1-V(E-H_0)^{-1}]$ is too computationally expensive to be practical. We recently learned that Bray and Stelbovics [40] solved this problem two decades ago by using efficient linear $Ax=b$ solvers, where $A=[1-V(E-H_0)^{-1}]$, $x=T(E)$, and $b=V$. To perform our calculations, we incorporate the techniques of [40, 46, 51, 55–57], which are summarized in the supplemental material.

Results.– The rest of the letter demonstrates the importance of all-order T-matrix, Coulomb interaction, and quantum electrons for three cases: neutral hydrogen, He-like magnesium, and H-like oxygen lines. These cases are chosen due to recent concerns [14, 19, 20, 54]. Additionally, these cases give insight on which approximations are valid for neutral and highly-ionized radiators.

First, accuracy of hydrogen line shapes is investigated for its importance for stellar modeling, in particular white dwarfs [58] and increasing concerns in their accuracy have been raised. There are inconsistencies between measured and modeled line shapes [59, 60], which questioned the accuracy of the existing calculations. Additionally, there is some uncertainty in modeling Lyα line shapes [61]. Lastly, Iglesias [54] suggested that quantum line-shape calculation might be necessary even for neutral hydrogen.

Figure 1a shows Lyβ hydrogen line shapes calculated under different approximations: 2^{nd}-order+dipole (dot-dashed orange), 2^{nd}-order+Coulomb (dotted green), all-order+dipole (dot-long-dash blue), and all-order+Coulomb (solid red); all calculations used quantum electrons. The red curve is the most accurate one without the three approximations. By comparing the three-approximated line shapes to the one without (red), we found that 2^{nd}-order is inaccurate, having twice the width of all-order. The comparison also suggests that dipole approximation is sufficiently accurate as long as it is computed in all-order.

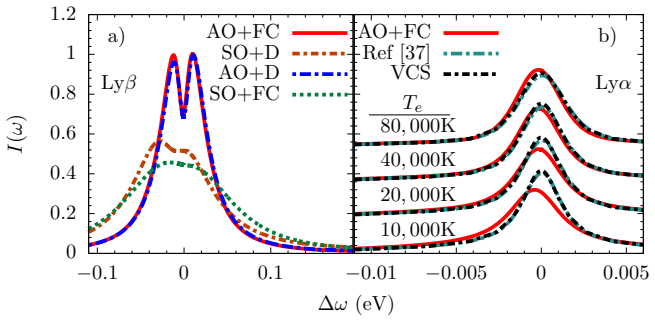

FIG. 1. a) Comparison of different approximations for H Lyβ at $T_e=1$ eV and $n_e=10^{18}e/\text{cm}^3$: SO+D is second-order with dipole; AO+D is all-order with dipole; SO+FC is second-order+full Coulomb; and AO+FC is all-order+full Coulomb. b) Comparison of Lyα calculations between this work and VCS [49] and Ref. [37] at $n_e=10^{18}e/\text{cm}^3$ with different temperatures; correspondence is achieved at high temperatures, but not at low temperatures.

Next, we investigate the importance of quantum effects for Lyα. In Fig. 1b), we compared our best calculations (red) with classical calculations (black and green). According to the correspondence principle [62], quantum effects would be important for low quantum number (e.g., Lyα) at low temperatures. The black curve is computed with the Vidal-Cooper-Smith (VCS) model [49], which is semi-analytic calculation done with classical electrons. The green curve is a classical particle simulation *Xenomorph* [36, 37]. Both classical calculations give identical results at all temperatures considered here. At $T_e=80,000$K, our quantum calculation agrees with the classical calculations. However, as the T_e drops, the quantum calculations becomes much broader than the classical calculations, proving the importance of quantum effects at low temperatures.

Fig. 2a) shows that, at $T_e=10,000$K, the wing of the Lyα opacity is higher than VCS by up to 50% due to the extra broadening caused by the quantum effects. The line wings are important for Rosseland-mean-opacity calculations, and this may have notable impact on stellar modeling and spectroscopy [10]. Preliminary investigations with the TLUSTY atmosphere code [63] show that the increase in the opacity of Lyα changes the model spectra by more than the uncertainties for spectral calibrations [64, 65]; see Fig. 2c). Detailed analysis is beyond the

scope but should be investigated in near future.

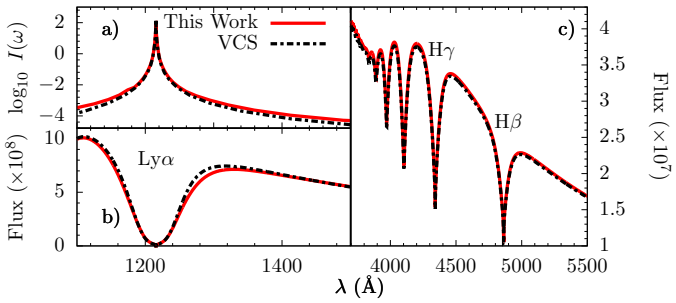

FIG. 2. a) Comparison of wing behavior between our new calculation and VCS. b) Emergent white dwarf spectrum with new Lyα line shapes. c) Same as b) but focusing on the visible. The visible flux is raised beyond previously-estimated uncertainties because of the broader Lyα profile.

We also investigated the impact of each approximation for a highly-ionized radiator. The magnesium Heγ line ($n = 1 \rightarrow 4$) is of particular interest due to its use as a density diagnostic in the iron-opacity experiments [18]. Nagayama *et al.* [20] showed that the inferred densities depend significantly on the choice of line-shape models. Two of the most commonly used line-shape codes, TOTAL and MERL, infer electron densities that differ by nearly 70%. TOTAL and MERL use different electron broadening models, Lee [66] and O'Brien and Hooper [67] (hereafter OH), respectively, which use different approximations.

To understand the impact of the electron-broadening models, Iglesias [19] investigated how much difference is caused by the electron-broadening models. Iglesias [19] showed that Lee electron-broadening model better reproduces neutral hydrogen experimental data [29] while OH overpredicts the measured widths. This extra broadening could be caused by OH neglecting strong collisions [4, 50]. However, the result is not conclusive because both calculations still use both 2^{nd}-order and dipole approximations.

Our work here can refine this investigation by removing the limiting approximations used by Lee and OH. For this comparison, we use the same basis set as Iglesias [19] so that any differences are solely due to electron-broadening models.

First we test our understanding of Lee (dashed purple) and OH (dashed black) from Iglesias [19] by reproducing them (Fig 3a) with similar approximations. These were computed at T_e = 180eV and $n_e = 3.1 \times 10^{22} e/\text{cm}^3$, and the line shapes are convolved with the instrument width ($\lambda/\Delta\lambda$ = 1000). To reproduce the Lee model in [19], we used 2^{nd}-order approximation and retained only the dipole term of the full-Coulomb interaction. For our implementation of the OH model, we used 2^{nd}-order, the dipole interaction (6) and set the screening length to infinity. We show that our model can reproduce Lee and OH results by introducing similar approximations.

Now, we remove the remaining approximations and compare our best calculations (red) with the Lee and OH models. We find that the width of the calculation is between those of Lee and OH. Also, our calculation exhibits the red shift previously explored in Junkel *et al.* [53], which is not present in either Lee or OH.

Based on our preliminary investigation of Heγ line, the true density could be roughly 30% higher than reported in [18]. Determination of the temperature and density of [18] requires careful analysis involving multiple lines with multiple sources of errors to be propagated, which is the beyond the scope of this paper. However, it is likely that the refined line shapes suggest the true density to be significantly higher than Ref. [18]. The model-data iron-opacity discrepancies need to be revisited at the refined temperature and density to understand the radiation-transport puzzle in the Sun.

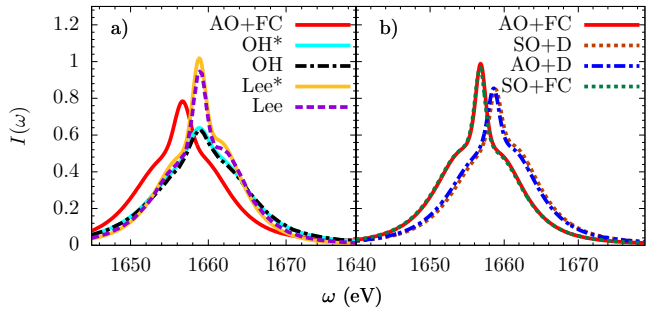

FIG. 3. Comparison of Mg Heγ ($n = 1 \rightarrow 4$) line-shape models at T_e = 180eV and $n_e = 3.1 \times 10^{22} e/\text{cm}^3$. a) Comparison of our work against Lee [66] and OH [67] plus our attempts to reproduce each calculation, indicated by the * for each model; line shapes here are Doppler and instrument [18] convolved. b) Same as Fig. 1a) but for Mg Heγ (same legend). Contrary to hydrogen, 2^{nd}-order is valid, but the full-Coulomb is necessary, causing the redshift that is not present in either Lee or OH.

To understand what approximations are important for highly-ionized radiators, we compared calculations with different approximations (Fig. 3b) with the same color scheme as Fig. 1a. Contrary to hydrogen, we found that the 2^{nd}-order calculation is sufficiently accurate for highly ionized line shapes; this is confirmed for the very first time. Additionally, we found that the dipole approximation is inaccurate, full Coulomb treatment is needed. The redshift and asymmetries are introduced by the monopole contribution to the Coulomb interaction.

It has been well established that the including the frequency dependence of the broadening (equivalent to including "off-shell" [68] components in the T-matrix, as we have done here) affects line shapes in a measurable way [29]. Figure 4 demonstrates how neglecting the frequency dependence can alter the spectrum of

H-like oxygen at solar interior conditions (T_e = 180eV, $n_e = 3 \times 10^{23} e/\text{cm}^3$). This example was chosen due to its potential importance for the stellar opacity problem [18]. The frequency-dependent T-matrices gives structure to the wings of Lyα. Additionally, the opacity is raised between Lyα and Lyβ and affects the intensity of the high-n lines. This example suggests potential impact on the solar-opacity work because oxygen is the biggest opacity contributor and the Rosseland-mean weighting function peaks around 700eV [69].

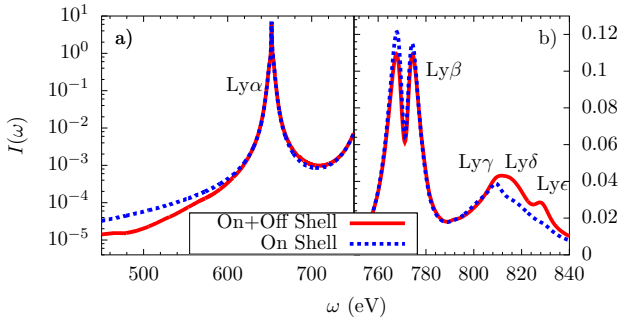

FIG. 4. Comparison of O VIII calculations at T_e = 180eV and $n_e = 10^{23} e/\text{cm}^3$ that include and neglect the frequency dependence in the calculated T-matrices for a) Lyα and b) Lyβ, Lyγ, Lyδ, and Lyϵ. The frequency-dependent T-matrices result in decreased opacity in the red wing of Lyα, but raised opacity between Lyα and Lyβ and more intense Lyδ and Lyϵ transitions.

Summary.—We removed three long-standing line-shape approximations (dipole, semi-classical, and 2^{nd}-order) simultaneously for the first time and investigated its impact on neutral hydrogen and high-ionized magnesium line shapes. These calculations not only provide the most theoretically-sound line-shapes but also revealed that different approximations are important for the two cases. For hydrogen, 2^{nd}-order and semi-classical approximation can change the line width by 50% at some conditions, which can affect white dwarf modeling and diagnostics. For magnesium, commonly used dipole approximation with an ad-hoc strong-collision correction would underestimate the magnesium Heγ width by 15% without introducing the necessary line shift. This can have notable impacts on the determination of the density of laboratory plasmas [20]. We also demonstrate the need for detailed line-shape calculations on oxygen opacity, where off-shell T-matrices lead to substantial changes in the spectra. While we only explore these examples, the importance of detailed line-shape calculations extend to other elements and transitions [70]. While we removed three major approximations, other improvements could still be made. For example, in this work, we use Debye screening; this will fail at high plasma coupling and a more accurate screening prescription will be needed. Line-shape theory refinements and benchmark experiments should continue to refine our understanding of atomic interaction with HDM.

We would like to thank S. B. Hansen and J. E. Bailey and K. Beckwith for comments on the manuscript. Sandia National Laboratories is a multimission laboratory managed and operated by National Technology and Engineering Solutions of Sandia, LLC., a wholly owned subsidiary of Honeywell International, Inc., for the U.S. Department of Energy's National Nuclear Security Administration under contract DE-NA-0003525. The work of T.G. and T.N. was performed under a Laboratory Directed Research and Development program at Sandia National Laboratories. The work of M.Z., C.F., and D.K. was carried out under the auspices of the US Department of Energy by Los Alamos National Laboratory under contract No. 89233218CNA000001. P.C., B.D., M.H.M., and D.E.W. acknowledge support from the United States Department of Energy under grant DR-SC0010623 and the Wootton Center for Astrophysical Plasma Properties under the United States Department of Energy collaborative agreement DE-NA0003843. I.B. acknowledges the Australian Research Council and the support of the National Computer Infrastructure and the Pawsey Supercomputer Centre. The views expressed in the article do not necessarily represent the views of the U.S. Department of Energy or the United States Government.

* thogome@sandia.gov

[1] C. A. Iglesias, F. J. Rogers, and B. G. Wilson, ApJL **322**, L45 (1987).
[2] I. Hubeny and T. Lanz, "Non-LTE line blanketed model atmospheres of hot, metal-rich white dwarfs," in *White Dwarfs*, Vol. 443, edited by D. Koester and K. Werner (1995) pp. 97–107.
[3] P. Bergeron, F. Wesemael, and G. Fontaine, Astrophys. J. **367**, 253 (1991).
[4] H. R. Griem, *Spectral line broadening by plasmas* (New York, Academic Press, Inc. (Pure and Applied Physics. Volume 39), 1974. 421 p., 1974).
[5] C. J. Keane, B. A. Hammel, D. R. Kania, J. D. Kilkenny, R. W. Lee, A. L. Osterheld, L. J. Suter, R. C. Mancini, J. Hooper, C. F., and N. D. Delamater, Physics of Fluids B **5**, 3328 (1993).
[6] B. A. Hammel, C. J. Keane, M. D. Cable, D. R. Kania, J. D. Kilkenny, R. W. Lee, and R. Pasha, Phys. Rev. Lett. **70**, 1263 (1993).
[7] D. G. Hummer and D. Mihalas, Astrophys. J. **331**, 794 (1988).
[8] J. C. Stewart and J. Pyatt, Kedar D., Astrophys. J. **144**, 1203 (1966).
[9] G. Ecker and W. Kröll, Physics of Fluids **6**, 62 (1963).
[10] I. Hubeny, A&A **86**, 225 (1980).
[11] M. A. Barstow, H. E. Bond, J. B. Holberg, M. R. Burleigh, I. Hubeny, and D. Koester, MNRAS **362**, 1134 (2005).
[12] S. O. Kepler, S. J. Kleinman, A. Nitta, D. Koester, B. G. Castanheira, O. Giovannini, A. F. M. Costa, and L. Althaus, MNRAS **375**, 1315 (2007).

[13] R. E. Falcon, D. E. Winget, M. H. Montgomery, and K. A. Williams, Astrophys. J. **712**, 585 (2010).

[14] M. A. Schaeuble, T. Nagayama, J. E. Bailey, T. A. Gomez, M. H. Montgomery, and D. E. Winget, Astrophys. J. **885**, 86 (2019).

[15] D. E. Winget, C. J. Hansen, J. Liebert, H. M. van Horn, G. Fontaine, R. E. Nather, S. O. Kepler, and D. Q. Lamb, ApJL **315**, L77 (1987).

[16] J. A. García, A. C. Fabian, T. R. Kallman, T. Dauser, M. L. Parker, J. E. McClintock, J. F. Steiner, and J. Wilms, MNRAS **462**, 751 (2016).

[17] T. Kallman, M. Bautista, J. Deprince, J. A. García, C. Mendoza, A. Ogorzalek, P. Palmeri, and P. Quinet, Astrophys. J. **908**, 94 (2021).

[18] J. E. Bailey, T. Nagayama, G. P. Loisel, G. A. Rochau, C. Blancard, J. Colgan, P. Cosse, G. Faussurier, C. J. Fontes, F. Gilleron, I. Golovkin, S. B. Hansen, C. A. Iglesias, D. P. Kilcrease, J. J. Macfarlane, R. C. Mancini, S. N. Nahar, C. Orban, J.-C. Pain, A. K. Pradhan, M. Sherrill, and B. G. Wilson, Nature (London) **517**, 56 (2015).

[19] C. A. Iglesias, High Energy Density Physics **18**, 14 (2016).

[20] T. Nagayama, J. E. Bailey, R. C. Mancini, C. A. Iglesias, S. B. Hansen, C. Blancard, H. K. Chung, J. Colgan, P. Cosse, G. Faussurier, R. Florido, C. J. Fontes, F. Gilleron, I. E. Golovkin, D. P. Kilcrease, G. Loisel, J. J. MacFarlane, J.-C. Pain, G. A. Rochau, M. E. Sherrill, and R. W. Lee, High Energy Density Physics **20**, 17 (2016).

[21] T. Nagayama, J. E. Bailey, G. P. Loisel, G. S. Dunham, G. A. Rochau, C. Blancard, J. Colgan, P. Cossé, G. Faussurier, C. J. Fontes, F. Gilleron, S. B. Hansen, C. A. Iglesias, I. E. Golovkin, D. P. Kilcrease, J. J. MacFarlane, R. C. Mancini, R. M. More, C. Orban, J. C. Pain, M. E. Sherrill, and B. G. Wilson, Phys. Rev. Lett. **122**, 235001 (2019).

[22] M. Baranger, Physical Review **112**, 855 (1958).

[23] U. Fano, Physical Review **131**, 259 (1963).

[24] T. Hussey, J. W. Dufty, and C. F. Hooper, Phys. Rev. A **12**, 1084 (1975).

[25] P. Kepple and H. R. Griem, Physical Review **173**, 317 (1968).

[26] E. W. Smith, J. Cooper, and C. R. Vidal, Physical Review **185**, 140 (1969).

[27] R. Stamm, E. W. Smith, and B. Talin, Phys. Rev. A **30**, 2039 (1984).

[28] E. Stambulchik and Y. Maron, J. Quant. Spec. Radiat. Transf. **99**, 730 (2006).

[29] W. L. Wiese, D. E. Kelleher, and D. R. Paquette, Phys. Rev. A **6**, 1132 (1972).

[30] T. L. Pittman and C. Fleurier, Phys. Rev. A **33**, 1291 (1986).

[31] S. Glenzer, N. I. Uzelac, and H. J. Kunze, Phys. Rev. A **45**, 8795 (1992).

[32] S. Glenzer and H. J. Kunze, Phys. Rev. A **53**, 2225 (1996).

[33] R. J. Peláez, C. Pérez, V. R. González, F. Rodríguez, J. A. Aparicio, and S. Mar, Journal of Physics B Atomic Molecular Physics **38**, 2505 (2005).

[34] M. A. Gigosos, V. Cardenoso, and F. Torres, Journal of Physics B Atomic Molecular Physics **19**, 3027 (1986).

[35] M. A. Gunderson, G. C. Junkel-Vives, and C. F. Hooper, J. Quant. Spec. Radiat. Transf. **71**, 373 (2001).

[36] T. A. Gomez, T. Nagayama, D. P. Kilcrease, M. H. Montgomery, and D. E. Winget, Phys. Rev. A **94**, 022501 (2016).

[37] P. B. Cho, T. A. Gomez, M. H. Montgomery, M. Fitz Allen, B. Hobbs, I. Hubeny, and W. D. E., "Simulations of Stark-Broadened Hydrogen Balmer Line Shapes for DA White Dwarf Synthetic Spectra," (2021), submitted.

[38] T. A. Gomez, T. Nagayama, D. P. Kilcrease, M. H. Montgomery, and D. E. Winget, Phys. Rev. A **98**, 012505 (2018).

[39] T. A. Gomez, T. Nagayama, C. J. Fontes, D. P. Kilcrease, S. B. Hansen, M. C. Zammit, D. V. Fursa, A. S. Kadyrov, and I. Bray, Phys. Rev. Lett. **124**, 055003 (2020).

[40] I. Bray and A. T. Stelbovics, Phys. Rev. A **46**, 6995 (1992).

[41] C. A. Iglesias, H. E. Dewitt, J. L. Lebowitz, D. MacGowan, and W. B. Hubbard, Phys. Rev. A **31**, 1698 (1985).

[42] C. J. Hooper, Physical Review **165**, 215 (1968).

[43] L. A. Woltz and C. F. Hooper, Jr., Phys. Rev. A **38**, 4766 (1988).

[44] B. A. Lippmann and J. Schwinger, Physical Review **79**, 469 (1950).

[45] N. Mott, H. Massey, and H. Massey, *The Theory of Atomic Collisions*, The International Series of Monographs on Physics (Clarendon Press, 1965).

[46] M. C. Zammit, D. V. Fursa, and I. Bray, Phys. Rev. A **82**, 052705 (2010).

[47] H. R. Griem, A. C. Kolb, and K. Y. Shen, Physical Review **116**, 4 (1959).

[48] H. Bethe, Annalen der Physik **397**, 325 (1930).

[49] C. R. Vidal, J. Cooper, and E. W. Smith, J. Quant. Spec. Radiat. Transf. **11**, 263 (1971).

[50] S. Alexiou, Phys. Rev. Lett. **75**, 3406 (1995).

[51] L. A. Woltz and C. F. Hooper, Jr., Phys. Rev. A **30**, 468 (1984).

[52] S. Alexiou, High Energy Density Physics **23**, 188 (2017).

[53] G. C. Junkel, M. A. Gunderson, C. F. Hooper, Jr., and D. A. Haynes, Jr., Phys. Rev. E **62**, 5584 (2000).

[54] C. A. Iglesias, High Energy Density Physics **35**, 100743 (2020).

[55] C. A. Iglesias, High Energy Density Physics **38**, 100921 (2021).

[56] R. D. Cowan, *The Theory of Atomic Structure and Spectra* (Los Alamos Series in Basic and Applied Sciences, Berkeley: University of California Press, 1981, 1981).

[57] T. Gomez, T. Nagayama, C. Fontes, D. Kilcrease, S. Hansen, M. Montgomery, and D. Winget, Atoms **6**, 22 (2018).

[58] P. Bergeron, in *NATO Advanced Science Institutes (ASI) Series C*, NATO Advanced Science Institutes (ASI) Series C, Vol. 403, edited by M. A. Barstow (1993) p. 267.

[59] P. E. Tremblay and P. Bergeron, Astrophys. J. **696**, 1755 (2009).

[60] M. H. Montgomery, R. E. Falcon, G. A. Rochau, J. E. Bailey, T. A. Gomez, A. L. Carlson, D. E. Bliss, T. Nagayama, M. Stein, and D. E. Winget, High Energy Density Physics **17**, 168 (2015).

[61] E. Stambulchik, High Energy Density Physics **9**, 528 (2013).

[62] N. Bohr, Zeitschrift fur Physik **2**, 423 (1920).

[63] I. Hubeny and T. Lanz, Astrophys. J. **439**, 875 (1995).

[64] G. Narayan, T. Matheson, A. Saha, T. Axelrod, A. Calamida, E. Olszewski, J. Claver, K. S. Mandel, R. C.

Bohlin, J. B. Holberg, S. Deustua, A. Rest, C. W. Stubbs, C. E. Shanahan, A. L. Vaz, A. Zenteno, G. Strampelli, I. Hubeny, S. Points, E. Sabbi, and J. Mackenty, ApJS **241**, 20 (2019).

[65] R. C. Bohlin, I. Hubeny, and T. Rauch, AJ **160**, 21 (2020).

[66] R. W. Lee, J. Quant. Spec. Radiat. Transf. **40**, 561 (1988).

[67] J. T. O'Brien and C. F. Hooper, Jr., J. Quant. Spec. Radiat. Transf. **14**, 479 (1974).

[68] M. Baranger, B. Giraud, S. K. Mukhopadhyay, and P. U. Sauer, Nuclear Physics A **138**, 1 (1969).

[69] J. E. Bailey, G. A. Rochau, S. B. Hansen, T. J. Nash, D. S. Nielsen, P. W. Lake, C. A. Iglesias, R. C. Mancini, J. J. MacFarlane, I. Golovkin, P. Wang, C. Blancard, P. Cosse, G. Faussurier, F. Gilleron, J. C. Pain, J. Abdallah, A. K. Pradhan, and S. N. Nahar, in *American Institute of Physics Conference Series*, American Institute of Physics Conference Series, Vol. 1161, edited by K. B. Fournier (2009) pp. 40–40.

[70] Line shapes of more complex atomic systems can be computed with this technique, though the additional number of electrons means that other techniques such as distorted wave will need to be implemented to reduce the computational effort. One limiting factor in more complex spectra will be memory requirements due to the sheer number of states in half-open atomic shells.